Research and development towards duty factor upgrade of the European X-Ray Free Electron Laser linac

J. Sekutowicz,[1] V. Ayvazyan,[1] M. Barlak,[3] J. Branlard,[1] W. Cichalewski,[2] W. Grabowski,[3] D. Kostin,[1] J. Lorkiewicz,[3] W. Merz,[1] R. Nietubyc,[3] R. Onken,[1] A. Piotrowski,[4] K. Przygoda,[2] E. Schneidmiller,[1] and M. Yurkov[1]

[1]*DESY, 22607 Hamburg, Germany*
[2]*TUL, 90-924 Łódź, Poland*
[3]*NCBJ, 05-400 Świerk, Poland*
[4]*FastLogic Sp. z. o. o., 90-441 Łódź, Poland*

(Received 10 June 2014; published 7 May 2015)

We discuss the progress in the R&D program for a future upgrade of the European XFEL facility, namely for an operation in the continuous wave (cw) and long pulse (lp) modes, which will allow for significantly more flexibility in the electron and photon beam time structure. Results of cw/lp runs with preseries XFEL cryomodules and status of components needed for the new operation modes are presented here.

DOI: 10.1103/PhysRevSTAB.18.050701 PACS numbers: 29.20.Ej, 41.60.Cr

I. INTRODUCTION

The European XFEL superconducting linac is based on cavities and cryomodules (CM) developed for the TESLA linear collider. The linac will operate nominally in short pulse (sp) mode with 1.35 ms rf pulses (750 μs rise time and 600 μs bunch train). With 222 ns bunch spacing and 10 Hz rf-pulse repetition rate, up to 27000 bunches per second will be accelerated to 17.5 GeV to generate uniquely high average brilliance photon beams at very short wavelengths [1]. While many experiments can take advantage of full bunch trains, others desire an increased intrapulse distance between bunches to several μs or short bursts with a kHz repetition rate. For these experiments, the high average brilliance can be preserved only when the duty factor (DF) is much larger than that for the nominal sp operation.

The goal of our studies is to prove feasibility of cw operation of the main linac at gradients E_{acc} up to approximately 7 MV/m. At higher gradients, we propose lp operation with DFs scaled proportionally to $(7/E_{\mathrm{acc}})^2$ to keep the total cryogenic load constant. The studies, initiated in 2005/2006, are motivated by the DFs which can be anticipated for superconducting accelerators. Unlike the European XFEL, large x-ray FEL facilities driven by room temperature linacs have very low DFs, much below 0.1%, and therefore even less flexibility in the photon beam time structure.

The present layout of the XFEL accelerator is shown in Fig. 1. Table I displays parameters of the accelerator subsections (L0, L1, L2 and ML) assumed for the cw/lp operation modes and an example of beam parameters. We should note here that in the upgrade scenario for new operation modes, which is later discussed in more detail, the ML has an additional 12 standard XFEL CMs, relocated from the injector section (IS). In this scenario, all 17 CMs in linacs L0, L1 and L2 will be replaced with new ones capable to operate in cw mode at gradients up to 15 MV/m. The new cryomodules should operate at the same gradients as the standard CMs in IS in the sp mode. This will guarantee high bunch quality for all three operation modes sp, lp and cw. Unlike in the IS none of the 96 ML cryomodules will require any modification.

This will substantially reduce investment for the proposed upgrade. Both the upgraded IS and the ML will need an additional cw operating rf system and a larger cryogenic plant.

In the sp mode, XFEL cavities will be fed by klystrons, which have maximum pulse duration of 1.38 ms resulting in a largest possible nominal DF of 1.38% at a 10 Hz repetition rate. With new operation modes we expect to gain significantly in DF at the cost of operation at lower

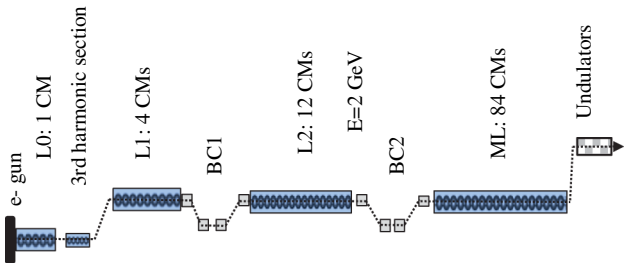

FIG. 1. Layout of the XFEL accelerator. Injector section up to 2 GeV and ML contains 17 CMs and 84 CMs respectively. BC1 and BC2 are bunch compressors.

TABLE I. XFEL accelerator parameters for cw/lp modes.

Parameter	Unit	
Injector section up to 2 GeV		
Number of CMs in linacs L0/L1/L2	...	1/4/12
Q_o of cavities in L0/L1/L2	[10^{10}]	2.5
1.8 K total load per CM in L0/L1/L2	[W]	91/45/80
E_{acc} for cw mode in linacs L0/L1/L2	[MV/m]	16/11/15
Main linac		
Number of CMs	...	96
1.8 K dynamic/static load per CM	[W]	16/4
Q_o of cavities	[10^{10}]	2.8
Maximum E_{acc} for cw mode	[MV/m]	7.3
Q_L, loaded Q of input coupler	[10^7]	~2
Mean rf-power P per cavity	[kW]	<2.5
Maximum peak rf-power P per cavity	[kW]	15
Assumed microphonics: (peak-peak)/2	[Hz]	32
Beam		
Charge per bunch	[nC]	0.5
Time between subsequent bunches	[μs]	4
I_{beam}	[mA]	0.125

gradients; however this does not exclude runs at very short wavelengths as discussed in [2].

There are technical and practical constraints for the DF upgrade of the XFEL facility.

II. CONSTRAINTS IN XFEL CW/LP MODES

A. Heat load at 1.8 K

One of the technical constraints is the heat load (HL) budget for the ML cryomodules, which in total (static plus dynamic heat) should not exceed approximately 20 W/CM at 1.8 K. Presently, the ML is split into seven 12-cryomodule long cryogenic strings and one will be added in the proposed upgrade scenario. The HL budget limitation results from a 72 mm diameter of the two-phase He transport tube (Fig. 2) and from its approximately 160 m length. The HL of 240 W per string is conservative. It has been assumed for all cryogenic strings in the ML to avoid a wavy flow of helium.

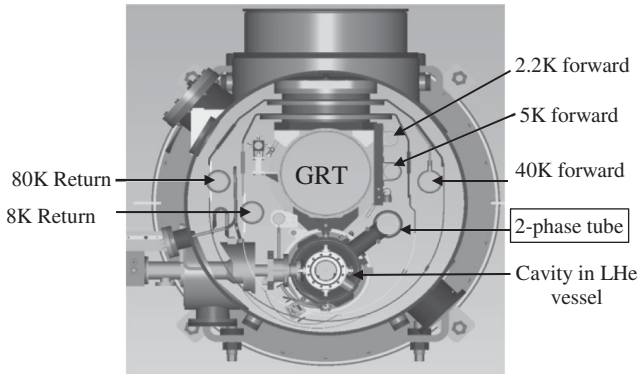

FIG. 2. Cross section of the XFEL cryomodule. GRT stands for gas return tube.

TABLE II. Capacity and HL of cryogenic plant.

T range	Nominal sp operation		Upgraded cw/lp operation	
[K]	Cap. [W]	HL [W]	Cap. [W]	HL [W]
2/1.8	2450	1175	4980	3320
5–8	4000	3510	8130	5430
40–80	30000	15300	61000	40700

B. Upgrade of the cryogenic plant

New 1.3 GHz cryomodules in the IS will have a larger diameter two-phase helium tube allowing for enhanced HL as listed in Table I. The heat load for all 17 CMs in the injector part will be approximately 1230 W. An additional heat load in the IS will be generated by a superconducting injector cavity and third harmonic cavities. The total heat load of the ML is estimated to be 1920 W. Table II shows the capacity (Cap.) of the present and upgraded cryogenic plants for three temperature ranges. The cryoplant will operate at 1.8 K after the upgrade. The capacity for the upgraded plant is by 50% higher than the expected heat load of the XFEL accelerator and it is similar to that of the existing CEBAF cryogenic refrigerator at JLab. The size of the upgraded cryoplant is still practical and should not cause excessive investment cost.

C. Compactness and efficiency of rf sources

Radio frequency power sources for the cw and lp operations will be installed in addition to the klystrons, feeding cavities in the sp mode. Having two rf systems, the XFEL will offer a unique flexibility in the time spectrum of the photon beam, being able to operate in all three modes. It is intended to have one rf source per cryomodule in the tunnel, which means the sources should be very compact. The required power per cryomodule will be approximately 120 kW. The new sources should be efficient, especially for the lp mode. These two properties, compactness and the lp mode efficiency, were arguments to initiate an R&D program for a high power inductive output tube (IOT). An IOT amplifier is very compact, as compared to present solid state amplifiers, and it takes power from the mains only when it delivers rf power, which makes it superior to cw-operating klystrons. The program was carried out by the American company CPI within the frame of the EUROFEL project. The first prototype was delivered to DESY in 2009 and is routinely used for the cw/lp cryomodule tests we will discuss later. The second prototype was ordered in 2012 and delivered to DESY in 2013. Measured parameters of both prototypes and target specifications are listed in Table III. The second prototype parameters are close to the target specifications. Figure 3 shows a picture of prototype I.

TABLE III. Parameters of IOT prototypes.

	Unit	Specification	Prototype I 2009	Prototype II 2013
F	[MHz]	1300	1300	1300
cw P_{out}	[kW]	120	85	105
Gain	[dB]	>22	22.3	22.7
Efficiency	[%]	>60	54	63
V_{beam}	[kV]	47–49	47–49	47–49

D. Heating of end groups

Originally the TESLA collider cavity and its auxiliaries were designed in the early 1990s for approximately 1% DF. In that design cavity end groups, containing two higher order mode (HOM) couplers and a coaxial fundamental mode (FM) coupler, are placed outside the liquid helium (LHe) vessel (Fig. 4). The arrangement has substantially reduced the fabrication costs, which was the main argument in the case of 22000 cavities needed for TESLA, but made end groups more sensitive to energy dissipation in couplers and to heat leaks. The design has proven since many years its capability to operate in sp mode at gradients up to 40 MV/m. In performance tests, when TESLA cavities are immersed vertically in superfluid helium without LHe vessel and HOM feedthroughs, gradients up to 45 MV/m were demonstrated in cw mode. When cavities are equipped with HOM antennas, the achieved gradients in performance tests are up to 40 MV/m for duty factors ~30%. After a TESLA cavity has been assembled in a cryomodule, only its body is directly cooled by superfluid helium. The end groups are cooled by means of heat conduction only. The DF limitation resulting from the cavity design is that heating of the end groups must not lead to quenching of cavity. The main sources of the heat are the antennas in HOM couplers, which are exposed to the residual magnetic field of the accelerating mode. New high thermal conduction feedthroughs were developed by Kyocera and will be used for all XFEL cavities to improve heat transfer from the HOM couplers. The feedthrough design follows developments carried out at TJNAF for the 12 GeV CEBAF upgrade [3]. In that design, the alumina window was replaced with a high-heat conduction sapphire window, which is brazed directly to a copper cylinder. The cylinder is connected to a two-phase tube with copper braids for better heat transfer to the 2 K environment. The feedthroughs and copper bridges are shown in Fig. 5.

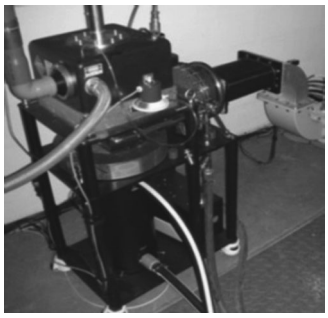

FIG. 3. First prototype of the 120 kW IOT at 1.3 GHz. Dimensions of the tube in frame are: $1.3 \times 0.6 \times 0.5$ [m].

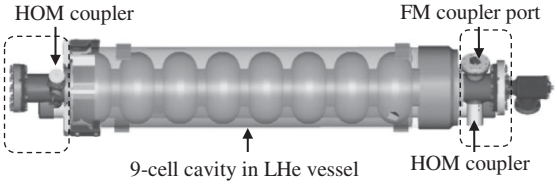

FIG. 4. TESLA cavity. End groups are marked with dashed lines.

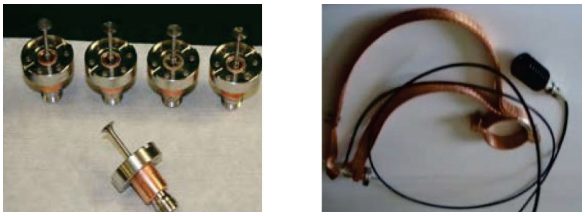

FIG. 5. New feedthroughs (left), copper braids (right) with feedthrough, cable and 50 Ω load.

New cw-operating cavities for the IS will have modified HOM couplers with shorter antenna, partially hidden in the output tube. Modeling of this modified HOM coupler showed that the retarded antenna is exposed to 50% less magnetic field than the antenna of the current design. This will significantly reduce heating. The magnetic field for the modified and the current HOM coupler is shown in Fig. 6.

The modified couplers will be also equipped with high conduction feedthroughs and braid thermal connections to the two-phase tube. Modeling of the HOM damping confirmed that the suppression of parasitic resonances did not change much for the new coupler and will be sufficient for all three operation modes, up to the nominal beam current of 4 mA in the sp mode (Fig. 7). The calculated damping will be verified with a copper model of a nine-cell cavity and then at 2 K with a Nb prototype.

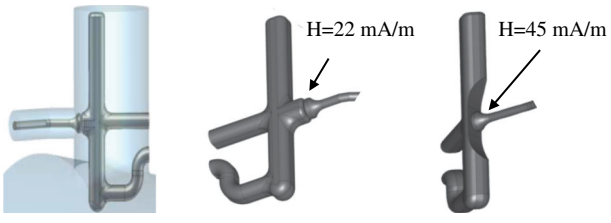

FIG. 6. Modified HOM coupler (left), magnetic field at the same stored energy for the modified coupler (mid) and current coupler (right).

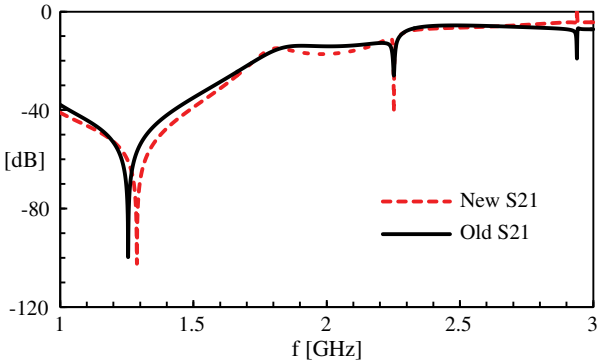

FIG. 7. Transfer functions of the new (red) and the current (black) HOM coupler. Note that the notches for the accelerating mode are not finally tuned to 1.3 GHz.

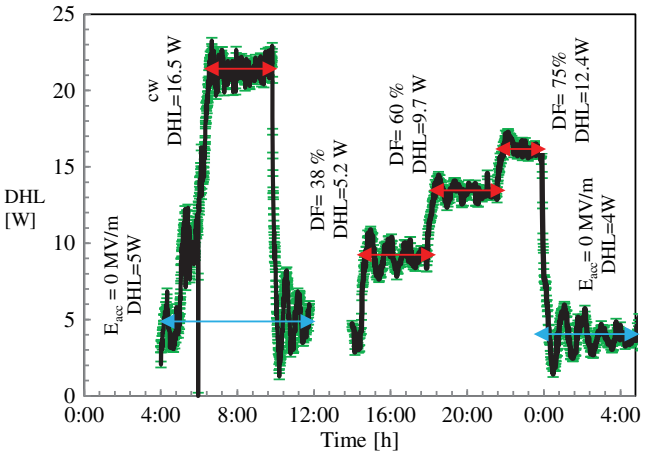

FIG. 8. DHL vs DF at E_{acc} of 5.6 MV/m. References at $E_{\mathrm{acc}} = 0$ MV/m are marked in blue.

III. TESTS OF PRESERIES CRYOMODULES

In summer 2011, we began tests with preseries XFEL cryomodules in order to identify the cw and lp operation limits for the XFEL main linac. The delivery of serial cryomodules began first in February 2014. We plan to test several of these cryomodules in the near future.

Eight runs were conducted up to now, each approximately one week long, with five preseries cryomodules. All tested cryomodules differed somewhat from XFEL series cryomodules, either because they housed cavities equipped with old type, low heat conduction HOM feedthroughs or, as for the cryomodule recently tested, because several cavities were made of large grain niobium, unlike standard XFEL cavities. We have partially presented these tests and the progress in developing other subsystems and components in [4–7].

We will discuss here four experiments in which we measured the dynamic heat load as a function of DF and E_{acc}. We should underline that, in all experiments, no irregular behavior of cryomodules like quenching, field emission or multipacting was ever observed.

A. Cryomodules housing fine grain cavities

1. Dynamic heat load vs DF

The first test we present here was conducted at 2 K. The cavities operated at 5.6 MV/m. The loaded quality factor, Q_L, for all cavities was adjusted to 1.5×10^7. In the tested CM (serial number PXFEL3_1), only three out of eight fine grain cavities were equipped with new feedthroughs and new thermal connections. The dynamic heat load (DHL) was measured for DF = 38, 60, 75 and 100% (cw). The test took 22 h. The cryomodule performed very stable over the entire test. Figure 8 shows DHL measured in that experiment. We measured DHL for $E_{\mathrm{acc}} = 0$ MV/m at the beginning and the end of the test. The result was 5 and 4 W respectively. It was shown in our previous tests that 0.2 W (green error bars in all following figures) is the smallest detectable DHL in the setup without any special measures. Oscillations, which mean values are depicted by arrows (red or blue) in all DHL diagrams, are due to the proportional integral differential controller of the Joule-Thomson valve. They do not contribute to the DHL uncertainty, but cause the time of the tests to be relatively long. The total superfluid helium consumption in the test stand is in all experiments determined by measured mass flow at very stable helium pressure of 16 and 30 mbar, corresponding to 1.8 and 2 K respectively. Knowing Q_o vs E_{acc} from the performance tests, for all cavities housed in PXFEL3_1, we could estimate dynamic heat load at all DFs. The estimated dynamic heat load for cavity n, EDHL_n, was calculated with formula $\mathrm{EDHL}_n = (V_n)^2 \mathrm{DF}/(R/Q)/Q_{o,n}$, where $V_n = l_c E_{\mathrm{acc}}$ is n cavity voltage, $l_c = 1038$ mm and $(R/Q) = 1012\ \Omega$ are respectively the length and beam impedance of the TESLA/XFEL cavity, and $Q_{o,n}$ is the intrinsic quality factor measured in performance tests. An estimated error in $\delta|Q_{o,n}|$ is $\lesssim$10% and depends mainly on the directivity of directional couplers and attenuation calibration of cables. The accelerating voltage V_n is determined by $(V_n)^2 = 4(R/Q)Q_{L,n}P_{\mathrm{for},n}$. The loaded quality factors $Q_{L,n}$ are measured directly with a network analyzer. The error in $Q_{L,n}$ is <3.5%. Input cavity power $P_{\mathrm{for},n}$ is measured with calibrated cables, directional couplers and power meters. Error in $P_{\mathrm{for},n}$ is maximally 4.7%. The total error in EDHL_n would be then $\pm$16%, however the error in EDHL, which is a sum of uncorrelated uncertainties for eight cavities is smaller by a factor of $1/\sqrt{8}$, and is $\pm$6.3%. The production tolerance on l_c is $\pm$3 mm, which contributes marginally to the error in calculated $E_{\mathrm{acc},n}$ from the V_n value. We will use the above error analysis for all experiments discussed here.

The PXFEL3_1 cavities showed in performance tests high intrinsic Qs, which mean value was $\langle Q_o \rangle = 2.2 \times 10^{10}$. EDHL vs DF is displayed in Table IV. The difference between measured and estimated DHL, shown in the last row, can be attributed to heating of the end groups.

TABLE IV. EDHL and end-groups heating at 2 K vs DF.

DF [%]	38	60	75	100
DHL [W]	5.2 ± 0.2	9.7 ± 0.2	12.4 ± 0.2	16.5 ± 0.2
EDHL [W]	4.2 ± 0.3	6.5 ± 0.4	8.3 ± 0.5	10.7 ± 0.7
End-groups heating [W]	1.0 ± 0.5	3.2 ± 0.6	4.1 ± 0.7	5.8 ± 0.9

TABLE V. EDHL and end-groups heating at 2 K vs E_{acc}.

E_{acc} [MV/m]	7.4	9.0	9.8	10.5	10.7
DHL [W]	4.5 ± 0.2	8.5 ± 0.2	11 ± 0.2	14.5 ± 0.2	16 ± 0.2
EDHL [W]	4.4 ± 0.3	6.8 ± 0.4	7.8 ± 0.5	9.3 ± 0.6	9.8 ± 0.6
End-groups heating [W]	0.1 ± 0.5	1.7 ± 0.6	3.2 ± 0.7	5.2 ± 0.8	6.2 ± 0.8

2. Dynamic heat load vs E_{acc}

The second test we want to discuss here was performed at 2 K and for DF = 20%. In that test, we measured DHL vs E_{acc}. As in the previous test, the Q_L of all cavities housed in the tested cryomodule (serial number PXFEL2_3) was adjusted to 1.5×10^7. The test was conducted for $E_{acc} =$ 7.4, 9.0, 9.8, 10.5 and 10.7 MV/m. The test duration was approximately 18 h.

The measured DHL is shown in Fig. 9. The mean value of intrinsic Q_o for cavities in that cryomodule was 2.0×10^{10}. The EDHL and the additional heat attributed to end groups are listed in Table V. In PXFEL2_3 only two cavities were equipped with new feedthroughs and new thermal connections.

The conclusion from these two tests, with PXFEL3_1 and PXFEL2_3, is that the heating of end groups contributes significantly to DHL and that it increases faster than proportionally vs DF and $(E_{acc})^2$. In either test, the heating amounts to approximately 6 W at maximum DF or highest E_{acc} respectively, causing a substantial reduction in the achievable gradient or/and duty factor for a 20 W budget.

B. Cryomodule housing seven large grain cavities

The recently tested cryomodule, XM-3, houses seven large grain (LG) niobium cavities and one polycrystalline cavity. LG cavities have cells made of large crystalline niobium. Their end groups are made of standard polycrystalline material. XM-3 was the first cryomodule in which all cavities were equipped with new HOM feedthroughs and new thermal connections. In all three tests we have conducted until now with this cryomodule, no heating of end groups was observed. This validated the concept of the high heat conduction feedthroughs and better cooling of HOM couplers by the attached copper braids. As before, the Q_L was adjusted to 1.5×10^7 for all XM-3 input couplers.

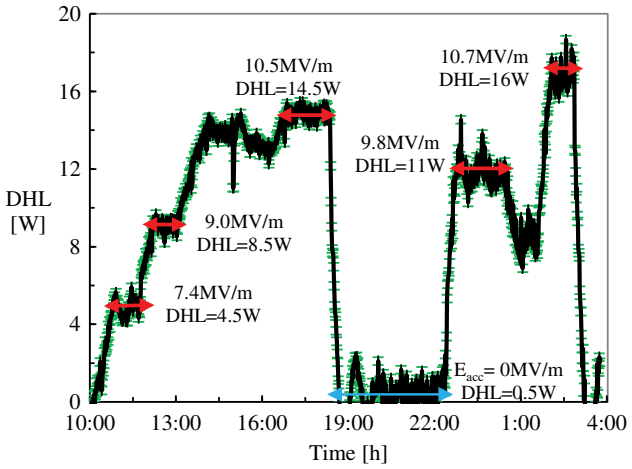

FIG. 9. DHL vs E_{acc} for DF of 20%. Reference at $E_{acc} =$ 0 MV/m is marked in blue.

1. Dynamic heat load vs E_{acc}; first fast cooldown

For the first cw experiment, XM-3 was cooled down fast, according to the standard DESY procedure. The rate was −3 K/ min beginning at 60 K down to 4.2 K. Figure 10 shows DHL at $E_{acc} = 7.0$ MV/m for 2 and 1.8 K, and at $E_{acc} = 9.5$ MV/m for 1.8 K. The test took 15 h, without 2 h and 30 min break for cooling down from 2 to 1.8 K. The mean value of $\langle Q_o \rangle$ in performance tests at 2 K for XM-3 cavities at 7 MV/m was 2.9×10^{10}, very close to 3.1×10^{10} measured in the cryomodule. It means that the string assembly did not degrade the performance and that there is no additional heating of end groups. After the temperature was lowered to 1.8 K, the dynamic heat load was measured

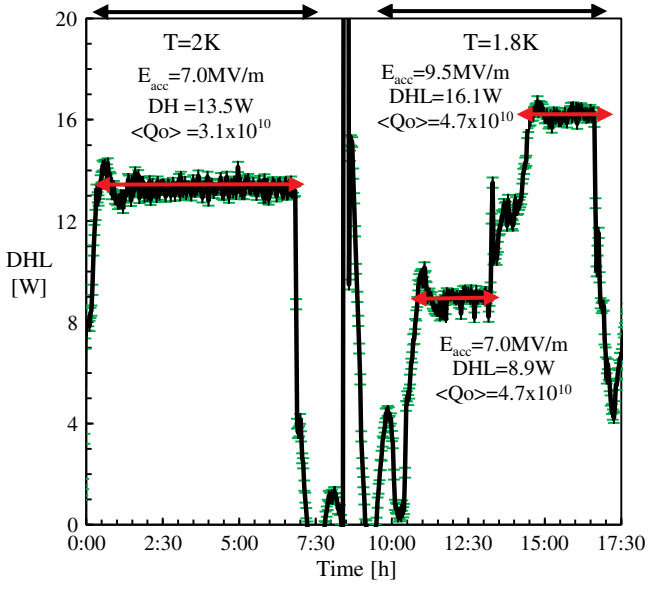

FIG. 10. DHL for $E_{acc} = 7.0$ and 9.5 MV/m; 2 K (left), 1.8 K (right). Reference for $E_{acc} = 0$ MV/m was DHL = 0 [W].

again at 7 MV/m and then at 9.5 MV/m. For both gradients, the measured $\langle Q_o \rangle$ was 4.7×10^{10}, by 52% higher than at 2 K. When the gradient was raised from to 9.5 MV/m the DHL increased proportionally to $(E_{\rm acc})^2$ by a factor of 1.84, however, for a typical curve Q_o $(E_{\rm acc})$ one would expect that DHL should increase slightly more. This observation will need more studies during next tests.

2. Q_o for slow cooldown

The second time the cryomodule was "parked" for 12 h at 10 K and then cooled down slowly to 4.2 K, with a rate of −0.01 K/ min. The measured $\langle Q_o \rangle$ at 2 and 1.8 K was reduced to 2.5×10^{10} and 3.3×10^{10} respectively. The result is a contradiction to what was reported by HZB [8], but confirmed observation at FNAL [9] for 1.3 GHz cavities, that a fast transition through critical Nb temperature T_c can improve Q_o.

3. Dynamic heat load vs $E_{\rm acc}$; second fast cooldown

In January 2014, XM-3 was cooled down for the third time. The cryomodule was kept at 15 K for 12 h and then cooled down at a rate of −4 K/ min to 4.2 K. As before, the dynamic heat load was measured both at 2 and 1.8 K. Figure 11 shows DHL measured at 2 K for 7.13 MV/m. This test took 5 h. Next, the cryomodule was cooled down to 1.8 K and DHL was measured at $E_{\rm acc}$ of 7.1, 8.3 and 10.2 MV/m (see Figs. 12 and 13). Each of these measurements took approximately 4 h. The second fast cooldown led again to high intrinsic quality factor, both for 2 and 1.8 K, confirming that the cooling rate, when passing through T_c, is the critical factor for the surface rf resistance. This time Q_o increased by 48% when XM-3 was cooled down from 2 to 1.8 K. The DHL measured at 7, 8.3 and 10.2 MV/m scaled again proportionally to $(E_{\rm acc})^2$, not showing the expected reduction in Q_o for typical dependence vs $E_{\rm acc}$. As in the two previous tests with XM-3, we did not observe an enhanced heating of the end groups and the cryomodule performed very stably in all three experiments.

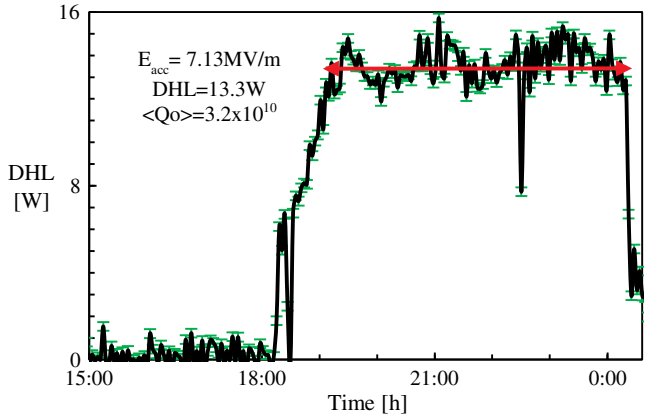

FIG. 11. DHL for $E_{\rm acc} = 7.13$ MV/m at 2 K after second fast cooldown. Reference for $E_{\rm acc} = 0$ MV/m was DHL = 0 [W].

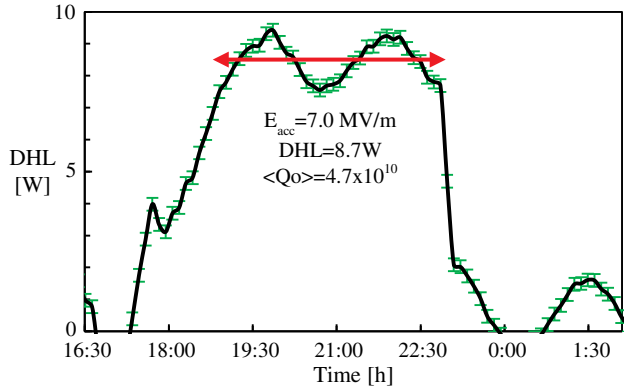

FIG. 12. DHL for $E_{\rm acc} = 7.0$ MV/m at 1.8 K after second fast cooldown. Reference for $E_{\rm acc} = 0$ MV/m was DHL = 0 [W].

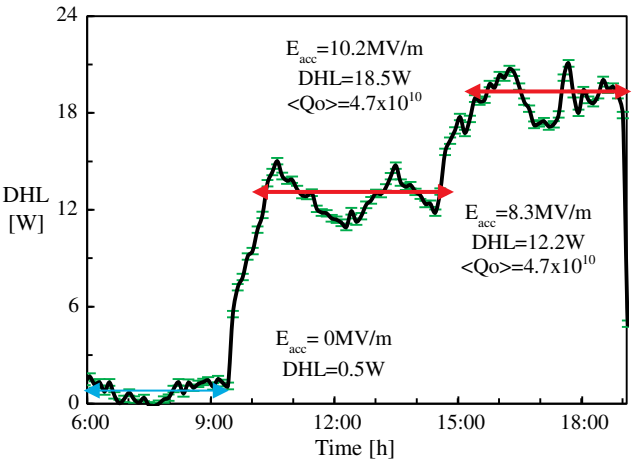

FIG. 13. DHL for $E_{\rm acc} = 8.3$ MV/m and 10.2 MV/m at 1.8 K after second fast cooldown. Reference for $E_{\rm acc} = 0$ MV/m was DHL = 0.5 [W].

IV. UPGRADE SCENARIO

The upgrade scenario mentioned earlier, with 136 new cw-operating TESLA-like cavities in the IS and 12 standard CMs relocated to the end of the ML, was discussed for the first time in [10] before testing XM-3. The experiments with XM-3 proved that no additional heating of the HOM couplers takes place with new output lines. Therefore, there is no need to reserve any part of the 20 W budget for these losses. The whole budget can now be devoted to the static and dynamic load.

The second change from our previous assumptions comes from the industrial production of the fine grain XFEL cavities. The mean Q_o, at 7–8 MV/m and 2 K for almost 200 tested cavities was 2.2×10^{10}, and it was higher

TABLE VI. Beam energy and DF estimated for the upgraded XFEL accelerator.

Operation mode	E_{beam} [GeV]	E_{acc} in ML [MV/m]	Beam-on DF [%]
sp (nominal)	19.8	23.4	0.6
cw	7.8	7.3	100
lp	10	10	53
lp	14	15	23

than what we had previously assumed. We can expect now, as shown in Table I, that the industry-produced ML cavities will have Q_o of at least 2.8×10^{10} when operated at 1.8 K. These new assumptions lead to new operation conditions displayed in Table VI, which shows final electron beam energy E_{beam}, gradient E_{acc} in the ML and the corresponding maximal beam-on DF for the upgraded XFEL accelerator. For the cw and lp operation examples listed in the table, DFs are remarkably larger than for the nominal mode presented in the first row.

Operation at $E_{\mathrm{acc}} = 7.3$ MV/m in the ML, resulting in an electron beam final energy of 7.8 GeV, should be possible for cw mode. At an E_{acc} of 10 MV/m in the ML, the electron beam will have a final energy of 10 GeV. The maximal expected beam-on DF for this gradient is 53%. According to recent studies [2], lasing to saturation at the fundamental wavelength in the baseline undulator is possible at 1 Å and below for this electron energy. It is also shown [11] that harmonic lasing is an attractive option for generating brilliant photon beams in x-ray FELs. This option would allow sub-Ångström operation of the European XFEL in cw mode at an energy of 7 GeV [2]. The last row of the table shows a projection for lp operation at an E_{acc} of 15 MV/m, not yet demonstrated in our experiments, for cryomodules housing eight fine grain cavities. With 15 MV/m in the ML, the electron beam will reach a final energy of 14 GeV, for which the wavelength of 1.5 Å was achieved at LCLS. The maximal expected beam-on DF at this E_{acc} is 23%.

The highest gradient achieved up to now in our tests was 14.7 MV/m during the first run in September 2013 with the XM-3 cryomodule. In that lp test at 1.8 K the mean intrinsic quality factor at 14.7 MV/m was 4.05×10^{10}. The test duration was 2 h and the measured DHL amounted to 10.4 W for DF of 25%. As in other tests, XM-3 performed very stably and no enhanced end-group heating was observed.

V. R&D FOR SRF PHOTOINJECTOR

We have continued, since 2006, an R&D program on a 1 mA-class all-superconducting electron photoinjector, envisioning its usefulness for the cw/lp operation modes and seeing this activity as an integral part of the XFEL DF-upgrade program. The injector is meant to generate bunches with normalized emittance below 1 μrad and charges up to 1 nC. Although, unlike other approaches, we propose to employ a superconducting lead (Pb) cathode, the most difficult task is the integration of the cathode into the superconducting cavity and its resistance to cleaning of the cavity. At the beginning of 2012 the cavity design was changed back to a version with the cathode plug, which allows avoiding exposition of the Pb film to acids used for the chemical treatment of cavities. Nonetheless, high pressure water rinsing, a mandatory final procedure to reach high gradients in a cavity, still causes problems. The plug cavity was built and tested for the first time at TJNAF by Kneisel. Figure 14 shows pictures of the cavity and its tests result with uncoated and coated plugs. In either test, the performance was very encouraging; even though the gradient reached on the cathode (E_{cath}) was only 38 MV/m for the Pb-coated plug, as compared to 54 MV/m in the baseline test with the uncoated Nb plug.

Later in 2012, the cavity was installed into a horizontal cryostat at HZB for cryogenic and quantum efficiency tests. The results were unsatisfactory in both cases. The maximum gradient reached on the cathode was 28 MV/m [12] with a significantly degraded intrinsic quality factor. The quantum efficiency of the Pb coating, measured without laser cleaning (no powerful laser was available for the test) was significantly lower, by a factor of approximately 20,

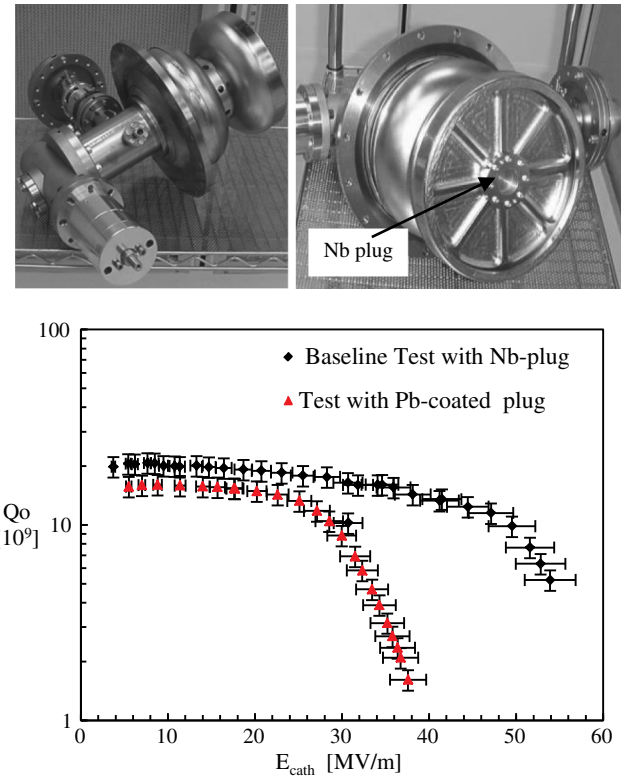

FIG. 14. Pictures and test result of the SRF gun 1.6-cell cavity; uncoated Nb plug (black), Pb coated plug (red).

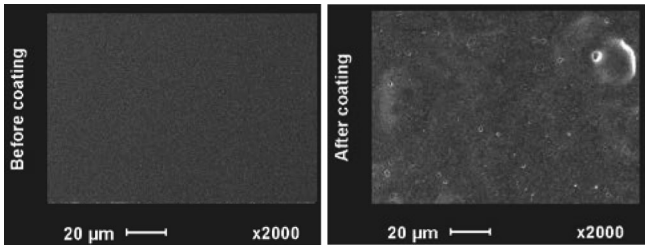

FIG. 15. Pictures of Nb samples before (left) and after coating (right). Scale (bar 20 μm) is shown in the lower left corners.

compared to what had been measured on the best Pb-coated samples after cleaning.

In 2013, the cavity was electropolished and tested at DESY for the first time, but we could not reproduce the good performance demonstrated at TJNAF.

The maximum gradient on the cathode with an uncoated Nb plug was only 29 MV/m. Our current explanation is that replacing the indium wire with an indium foil to seal the plug improved the reliability of the vacuum tightness but cooling of the plug deteriorated. We have modified the plug for better cooling by drilling and milling channels for superfluid helium in it. The next chemical treatment and cryogenic tests are scheduled for fall 2014 and 2015. To improve the quality of the Pb coating and its quantum efficiency, a second plug was mechanically polished and the roughness on the cathode surface was found to be less than 500 nm. The Pb coating will be done as before; an arc-deposition technique will be used with a filter removing droplets. An additional "smoothening" procedure with high intensity plasma pulses will be applied [13]. This technique has been tested on samples, which surface fragments before and after the coating are shown in Fig. 15. The sample before coating (left in the figure) is very smooth. After the coating and plasma treatment (right in the figure) small droplets were found. Their diameters did not exceed 25 μm and their height was below 7 μm. Compared to the plug assembled in the gun cavity investigated at HZB, the surface has much better uniformity and significantly less and smaller droplets. The QE test at BNL of the new Pb-coated plug, before it will be attached to the cavity at DESY, is scheduled for summer 2015.

VI. SUMMARY AND FUTURE PLANS

All cryomodule experiments conducted since 2011 are promising and show feasibility of the XFEL accelerator operation modes with substantially larger DFs. With doubling the capacity of the present XFEL cryogenic plant, to 5 kW at 1.8 K and with limiting the total heat load per CM to 20 W at 1.8 K in the main linac, the final electron beam energy of 7.8 GeV in the cw mode seems achievable. Higher energies are possible in the long pulse mode. The recently performed tests with the XM-3 preseries cryomodule proved that the new HOM couplers output lines and their thermal connections mitigate very effectively the additional heating of end groups and therefore the whole 20 W/CM budget can be devoted to the static and dynamic heat load only, allowing for higher operational gradient and/or for larger DF. We will continue the cryomodule tests in the near future with serial XFEL cryomodules, to gain statistics for components of the ML operating in the cw and lp modes. We would like to test in 2015, as an intermediate goal, serial CMs at 1.8 K to prove experimentally if operation of fine grain cavities at lower temperature is beneficiary and if projection of results acquired at 2 to 1.8 K is justified. Furthermore, lp operation of serial XFEL cryomodules at gradients higher than 14.7 MV/m will be of great interest, enabling pinpointing of maximum beam energy vs DF for the assumed heat load budget in the ML.

In addition, developments of other cw operating components like rf sources and electron source is well advanced. Their advancement showing promising results is discussed briefly here as an integral part of the XFEL upgrade R&D activity.

Two other R&D programs are in slow progress, for the third harmonic system (3.9 GHz) compensating the energy spread of bunches leaving the L0 linac and for the LLRF electronics. The 3.9 GHz cavities will need a similar modification as the 1.3 GHz cavities in the IS, to mitigate excessive heating of the end groups. The LLRF electronics, based on the μTCA architecture for XFEL operation in the sp nominal mode, needs further R&D to integrate rf and piezo feedbacks for cw/lp operation. This seems challenging at the moment, especially when several accelerating structures are supplied from a single rf source and the loaded quality factor is as high as or higher than 1.5×10^7.

All activities here discussed will be continued over the next years to support a final decision, scheduled for 2019, if the cw and/or lp operation of the XFEL facility is technically feasible and to help us with cost estimation for this upgrade. Synergy of the XFEL DF-upgrade and LCLSII project motivated us to conduct this R&D in collaboration with SLAC and FNAL.

ACKNOWLEDGMENTS

The authors would like to thank all colleagues at BNL, NCBJ, WUT, TUL, TJNAF and DESY for their scientific, engineering and technical support in the R&D programs presented here. We wish to express our gratitude to Katrin Lando for reading of the manuscript.

[1] TESLA XFEL Technical Design Report-Supplements No. DESY 2002-167 and No. TESLA- FEL 2002-09, Hamburg, 2002, edited by R. Brinkmann, B. Faatz, K. Flöttmann, J. Rossbach, J. Schneider, H. Schulte-Schrepping, D. Trines, T. Tschentscher, and H. Weise.

[2] R. Brinkmann, E. A. Schneidmiller, J. Sekutowicz, and M. V. Yurkov, Prospects for cw and lp operation of the European XFEL in hard x-ray regime, *Nuclear Instruments and Methods in Physics Research* ***A768****, 20 (2014)*.

[3] C. E. Reece, E. Daly, T. Elliott, J. P. Ozelis, H. L. Phillips, T. M. Rothgeb, K. Wilson, and G. Wu, High Thermal conductivity cryogenic RF feedthroughs for higher order mode couplers, in *Proceedings of the 21st Particle Accelerator Conference, Knoxville, TN, 2005* (IEEE, Piscataway, NJ, 2005).

[4] J. Sekutowicz, M. Ebert, F. Mittag, P. Kneisel, and R. Nietubyc, Test results of components for cw and near-cw operation of a superconducting linac, in *Proceedings of the 25th International Linear Accelerator Conference, LINAC-2010, Tsukuba, Japan* (KEK, Tsukuba, Japan, 2010).

[5] J. Sekutowicz, V. Ayvazyan, J. Branlard, W. Cichalewski, K. Czuba, M. Ebert, J. Eschke, A. Goessel, W. Jalmuzna, D. Kostin, W. Merz, F. Mittag, R. Onken, A. Piotrowski, K. Przygoda, J. Szewinski, and L. Zembala, Second cw and lp operation test of XFEL prototype cryomodule in *Proceedings of the 26th International Linear Accelerator Conference, LINAC-2012, Tel-Aviv, Israel* (SOREQ NRC, Tel-Aviv, Israel, 2012).

[6] J. Sekutowicz, Components for cw and lp operation of the XFEL Linac, in *Proceedings of the 4th International Particle Accelerator Conference, IPAC-2013, Shanghai, China, 2013* (JACoW, Shanghai, China, 2013).

[7] J. Branlard, W. Cichalewski, W. Jalmuzna, A. Piotrowski, K. Przygoda, J. Sekutowicz, and H. Schlarb, LLRF system design and performance for XFEL cryomodules cw operation, in *Proceedings of the International Conference on Superconducting Radio-Frequency, Paris, France, 2013* (CEA-Saclay, Saclay, France, 2013).

[8] O. Kugeler, Influence of cool-down on cavity quality factor, in *Proceedings of the International Conference on Superconducting Radio-Frequency, Paris, France, 2013* (CEA-Saclay, Saclay, France, 2013).

[9] A. Romanenko, A. Grassellino, O. Melnychuk, and D. A. Sergatskov, Dependence of the residual surface resistance of superconducting radio frequency cavities on the cooling dynamics around Tc, J. Appl. Phys. **115**, 184903 (2014).

[10] J. Sekutowicz, Feasibility of cw and lp operation of the XFEL linac, in *Proceedings of the 35th International Conference on Free Electron Laser, New York, USA* (BNL, Upton, USA, 2013).

[11] E. Schneidmiller and M. Yurkov, Harmonic lasing in x-ray free electron lasers, Phys. Rev. ST Accel. Beams **15**, 080702 (2012).

[12] T. Kamps, R. Barday, A. Burrill, A. Jankowiak, P. Kneisel, J. Knobloch, O. Kugeler, P. Lauinger, A. Neumann, R. Nietubyc, M. Schmeisser, J. Sekutowicz, J. Voelker, and I. Will, Results from beam commissioning of an SRF plug-gun cavity photoinjector, in *Proceedings of the 4th International Particle Accelerator Conference, IPAC-2013, Shanghai, China, 2013* (Ref. [6]).

[13] M. Barlak, High intensity plasma pulses in ceramic wettability improvement, *The Andrzej Soltan Institute for Nuclear Studies, 2010*.